Modeling of a novel multi-stage bubble column scrubber for flue gas desulfurization[☆]

B.C. Meikap [a], G. Kundu [b], M.N. Biswas [b,*]

[a] *Department of Chemical Engineering, Regional Engineering College, Rourkela 769008, India*
[b] *Department of Chemical Engineering, Indian Institute of Technology, Kharagpur 721302, India*

Abstract

Desulfurization of flue gases from various chemical industries in a techno-econo-enviro manner is a demanding technology. The concentrations of sulfur dioxide in and around these plants overshoot the danger point. In the present investigation, an attempt has been made for wet flue gas desulfurization using water as the absorbing medium in a newly developed scrubber. Prediction of SO_2 removal efficiency is very important for selection of pollution control equipment. The present paper reports on both the modeling and detailed experimental investigations on the scrubbing of SO_2 in the modified multi-stage bubble column scrubber (MMSBCS) using water. Experimental results show that almost 100% removal efficiency of SO_2, can be achieved in the present system without additives or pre-treatment. A comparison has been made between the predicted and experimental percentage removal efficiency of SO_2. Experimental results are in excellent agreement with the predicted values from the model.

Keywords: Flue gas; Wet scrubber; SO_2; Model; Absorption; Environment

1. Introduction

Bursting of bubbles in a bubble column is very important for high removal efficiency. Literature survey revealed that very few studies have been reported on the absorption of sulfur dioxide in water, using bubble columns of various conurations. Higbie [1] proposed the penetration theory based on Fick's one-dimensional unsteady diffusion for unsteady mass transfer at the gas–liquid interface. In unsteady cases, such as bubble growth and accelerating rising bubbles, Higbie's penetration theory is more suitable than those of Calderbank and Lochiel [2]. Shinner [3] developed a learning model as well as practical tool for easy estimation of the absorption rates for the absorption of SO_2 into aqueous solutions and slurries containing sulfites. Burman and Jameson [4] proposed mass transfer equations during bubble formation. They reported the mass transfer prediction from bubble to liquid surface during bubble formation.

Huckaby and Ray [5] reported studies on the absorption of SO_2 into growing or evaporating droplets of water. Han and Park [6] reported studies on the absorption of a single bubble of SO_2 into pure water. Terasaka and Tsuge [7] proposed a non-spherical bubble formation model. In the model, bubble shape, bubble surface area, bubble volume and gas chamber pressure during bubble formation can be predicted well.

Bronikowska and Rudzinski [8] proposed a model for the absorption of SO_2 based on the film theory of gas absorption and the chemical-equilibrium treatment of chemical reactions. Schmidt and Stichlmair [9] reported experimental investigations in spray scrubbers of different sizes with co-current flow of gas and liquid. This investigation highlighted the mass transfer units obtainable using SO_2 as one of the systems. The effects of the different operating variables and temperature on the mass transfer units were reported.

Bandyopadhyay and Biswas [10,11] developed a spray-cum-bubble column, which operates in both spray and bubble flow regimes. They reported theoretical modeling and experimental studies for absorption of SO_2 by water and dilute alkaline solution of sodium hydroxide. Their experimental results claimed a very high percentage removal of SO_2 (99–99.5%) by alkaline solution of sodium hydroxide. They also proposed a model for predicting absorption rate of SO_2 in water and sodium hydroxide solution.

Meikap et al. [12] developed a horizontal co-current ejector system for scrubbing of SO_2 by using water and alkaline solution. Their experimental results indicate that SO_2 can

Nomenclature

a	specific interfacial area per unit volume (m^2/m^3)
A	used for the gaseous constant
A^*	concentration of dissolved gas A at interface, in equilibrium with gas at interface $(kg\,mol/m^3)$
B	used for the liquid
C	liquid phase concentration $(kmol/m^3)$
C_{AL}^*	equilibrium concentration of A (at $z = 0$) $(kmol/m^3)$
C_{BO}	concentration of reactant B in bulk of solution $(kg\,mol/m^3)$
$C_{SO_2,i}$	inlet concentration of sulfur dioxide (ppm)
$C_{SO_2,o}$	outlet concentration of sulfur dioxide (ppm)
C_1	constant
D	diffusivity (m^2/s)
D_a	Damkohler number $((K_1 \Phi_L L / V_L))$
D_C	diameter of bubble column (m)
D_G	dispersion coefficient, gas phase (m^2/s)
D_H	diameter of expansion, contraction disks (m)
D_L	dispersion coefficient, liquid phase (m^2/s)
f	functions of variables
g	acceleration due to gravity (m/s^2)
G	molar flow rate of reacting diluent gas $(g\,mol/s)$
Ga	Galilei number, $gD_C^2 \rho_L^2 / \mu_{eff}^2$
G'	molar flow rate of inert gas $(g\,mol/s)$
H	height of the bubble column (m)
H_B	bubbling bed height (m)
H_e	Henry's law constant $(cm^3\,atm/g\,mol)$
H_R	height to diameter ratio of the bubble column
H_S	quiscent liquid height (m)
J	moles of B reacting with one mole of A (mol/mol)
k_{La}	volumetric mass transfer coefficient (s^{-1})
k_{LR}	$\sqrt{D_A k_2 C_{BO}}$, coefficient of chemical absorption (cm/s)
K_A	equilibrium constant (mole)
K_b	backward reaction rate constant (s^{-1})
K_B	equilibrium constant (mole)
K_f	forward reaction rate constant (s^{-1})
K_I	stoichiometric second ionisation constant $(g\,mol/l)$
K_L	liquid film mass transfer coefficient, for physical absorption (m/s)
K_{pq}	specific reaction rate constant for pth and qth order reaction $((mol/m^3)^{1-p-q}/s)$
K_W	ionic product of water $(g\,mol/l)^2$
K_1	first order reaction rate constant (s^{-1})
K_2	second order reaction rate constant $(cm^3/g\,mol\,s)$
L'	characteristic length (m)
$\sqrt{M}$	parameter in Eq. (8)
MMSBCS	modified multi-stage bubble column scrubber
N	number of data or sample size
pth	order of reaction with respect to A
P	pressure (N/m^2)
ΔP_i	pressure drop for gas–liquid flow $(i = 1, 2, \ldots)$ (N/m^2)
Pe_G	gas phase Peclet number $(V_G L / \Phi_G D_G)$
Pe_L	liquid phase Peclet number $(V_L L / \Phi_L D_L)$
q	which penetrates into the exhaust $(q = 1 - \eta_T)$
qth	order of reaction with respect to B
Q_G	volumetric flow rate of gas $(N\,m^3/s)$
Q_L	volumetric flow rate of liquid (m^3/s)
$-r_A$	rate of reaction of A $(-dC_A/dt)$ $(mol/m^3\,s)$
r, θ	radial and tangential direction
R	gas constant $(N\,m/kmol\,K)$
R	rate of absorption per unit area $(g\,mol/cm^2\,s)$
R_a	rate of absorption per unit volume $(kg\,mol/m^3\,s)$
Sh	Sherwood number $(Sh = k_{La} D_C^2 / D_L)$
St_G	Stanton number $(St_G = (K_L a \sqrt{1 + M} L / V_G) (RT/H_e))$ gas phase
St_L	Stanton number $(St_L = (K_L a \sqrt{1 + M} L / V_L))$ liquid phase
T	temperature $(^\circ C)$
T_{av}	average temperature $(^\circ K)$
V	operating scrubber volume (m^3)
V_G	gas velocity (m/s)
V_L	liquid velocity (m/s)
V_T	total system volume (m^3)
x	any axial distance from bottom of the column (m)
x_A	mole fraction of reactant A at any axial distance x
x_{A0}	initial mole fraction of A
$x_1 - x_{N+1}$	grid points
$\bar{x}$	reduced mole fraction $(\bar{x} = x_A / x_{A0})$
y_i	CO_2 concentration at the inlet (mol%)
y_o	CO_2 concentration at the outlet (mol%)
y'	first derivatives, dy/dx
y''	second derivative, d^2y/dx^2
$\bar{y}$	liquid phase concentration $(\bar{y} = C_{AL} C_{AL}^*)$
z	length $(z = x/L')$

Greek letters

Φ_L	fractional liquid phase hold up $(\Phi_L = 1 - \Phi_G)$
η_{SO_2}	removal efficiency of sulfur dioxide, from SO_2–air mixture
η_T	overall collection efficiency, for all three stages

η_1–η_3	individual stage efficiency
μ_{eff}	effective viscosity of liquid (kg/m/s)
μ_G	gas viscosity (kg/m/s)
μ_L	liquid viscosity (kg/m/s)
v_r	radial velocity (m/s)
v_z	axial velocity (m/s)
v_θ	tangential velocity (m/s)
ρ_G	gas density (kg/m^3)
ρ_L	liquid density (kg/m^3)
σ_L	liquid surface tension (N/m)

Subscripts

A	component A
aq	aqueous solution
b	backward
B	bubbling
f	forward
G	gas
I	ionization
L	liquid
SO_2	sulfur dioxide
$SO_{2,i}$	inlet concentration of SO_2
$SO_{2,o}$	outlet concentration of SO_2

be scrubbed from lean gas mixture by water with a removal efficiency exceeding 98.62%. In addition they reported that 100% removal of SO_2 could be achieved by alkaline solution from rich gas mixtures, by using alkaline scrubber.

Terasaka et al. [13] proposed a theory for SO_2 bubble formation at an orifice submerged in water. They also proposed a model for predicting bubble shape, bubble volume at the point of its detachment from an orifice, growth rate and mass transfer rate at the gas–liquid interface.

Glomba and Michal [14] reported a method for removing sulfur dioxide and fly ashes from boiler flue gases. Dohmann et al. [15] reported a process for removal of pollutants and trace impurities from flue gas, especially incinerator flue gas. De-dusting and absorption in a wet scrubber removed pollutants.

Critical analysis of the literature revealed that very few studies on the absorption of SO_2 in bubble column have been reported. Even though different wet scrubbers in various types and configurations have been suggested for the absorption of sulfur dioxide by either water or sodium alkalis. Their widespread commercial deployment has been few and far between. From a purely theoretical stand point it is expected that bubble breakup and regeneration of the dispersed medium would provide a large surface area in the form of discrete bubbles and that such a surface traveling through the liquid would be ideal for the absorption of soluble gases. In practice, however, simple bubble column have not met with the favor that the existing theory would apparently justify. However, more recently bubble columns are finding increasing favor for air pollution abatement systems, for handling both particulate and gases in one single step. In the recent industrial applications, the trend appears to be away from complex contactors with mechanical agitation or complex internal components, which may offer high pressure drop and sites for the deposition of solids, in the form of scale.

Measurements by laboratory units, mostly made using single bubble of known size, have verified the existence of high absorption rate, under certain operating conditions. The unpredictability of bubble column operation may, therefore, be attributed to the inadequacy of the existing theories in predicting bubble column performance. In addition, most laboratory investigations on absorption of SO_2 in water, have chosen to neglect liquid side resistance, while determining the mass transfer coefficient. This is a serious inadequacy, since SO_2 water systems are known to have controlling resistances in both the gas and the liquid sides. On the other hand, the reports from commercial units mainly deal with empirical correlation for predicting SO_2 removal efficiency, without attempting to develop any understanding of the fundamental process of bubble absorption.

In the present investigation, therefore, an attempt has been made to develop a generalized theoretical model, for predicting the performance of a bubble column scrubber with a view to attain definite insight into the process of absorption of SO_2 in water. The proposed model takes into consideration, the concentration distribution of SO_2 and the mixing dynamics of bubble movement. It attempts to predict the removal efficiencies of SO_2 as a function of bubble size and velocities, gas and liquid flow rates and tower height.

2. The theoretical model for the de-sulfurization of flue gas in a modified multi-stage bubble column scrubber

A bubble column can be considered as a system where a large number of gas bubbles are contacted with a continuum liquid. The soluble components from the gas phase are transferred to the liquid phase by continuous counter-current contact of the two phases as the swarm of bubble flow upward and the liquid flow downward. The actual flow situation is very complex and normally defies mathematical interpretation.

In all, the literature described earlier, a bubble is assumed to be always spherical because of simplification. However, deformation of bubble shape during bubble formation is obvious and the estimation of bubble surface area is very important for the study of mass transfer.

In the present work, a simple and realistic model of the bubble column performance is proposed on the basis of axial dispersion model. The axial dispersion model characterizes the back mixing in a column by simple one-dimensional Fick's-law-type diffusion equation. The

constant of proportionality in this equation is commonly known as the axial dispersion coefficient (D_L). The assumption that all the mixing processes follow a Fick's-law-type diffusion equation, regardless of the actual mechanism, becomes increasingly dubious with large degrees of back mixing. However, since the model characterizes the back mixing by only a single parameter, its simplicity has made it the most widely-used model. In axial dispersion model, all the individual mixing phenomena taking place in each phase are lumped into a dimensionless form as the Peclet number, $Pe(V_L/D_L)$. The value of Peclet number denotes the degree of back mixing. If $Pe \rightarrow 0$, back mixing is complete and for $Pe \rightarrow \alpha$, plug flow prevails.

For a multi-phase reactor, the back mixing in each phase is considered separately. In a bubble column (gas–liquid reactor), a considerably different degree of back mixing can exist in each phase. Furthermore, the back mixing increases with the diameter of reactor (i.e. usually more back mixing occurs in commercial reactors than in pilot-scale). In small-scale reactors, the gas-phase is usually assumed to move in plug flow with small back mixing. The standard axial dispersion model is a one-dimensional model that neglects the contributions of radial dispersion as well as non-uniform velocity distribution.

In the proposed model, to simplify the analysis of the bubble column (operating in a countercurrent mode of gas and liquid) the following assumptions have been made.

1. No reaction takes place in the gas phase.
2. The flow systems at the column are one-dimensional.
3. No radial (or tangential) change of properties/concentrations i.e. any radial dispersion.
4. Steady-state condition.
5. Relatively small partially back-mixed gas.
6. Partially back-mixed liquid.
7. Tower diameter to height ratio of the column is small.
8. Isothermal condition throughout the column (due to small amount of gas absorption, change in temperature is very small).
9. Dispersion coefficients of gas and liquid phase are not function of concentration.
10. The thermal capacity of the liquid in the system being very high, any heat generated by the wall friction of gas and compression, if any will not have any affect.
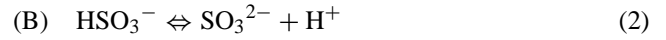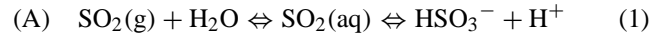
2.1. Model equations

Considering a bubble column in which the dispersed phase (i.e. the gas phase, sulfur dioxide–air mixture) flows in the upward direction against a continuous phase (i.e. the liquid flows opposite to the gas phase). Writing the material balance equation on each phase has developed a series of model equation.

However, before performing the material balance, the kinetics of the sulfur dioxide absorption by water has been discussed.

2.1.1. Kinetics of sulfur dioxide absorption in water

2.1.1.1. Reaction scheme. When sulfur dioxide is absorbed into water, the following reactions occur in the liquid phase:

$$(A) \quad SO_2(g) + H_2O \Leftrightarrow SO_2(aq) \Leftrightarrow HSO_3^- + H^+ \quad (1)$$

$$(B) \quad HSO_3^- \Leftrightarrow SO_3^{2-} + H^+ \quad (2)$$

The equilibrium constants for reaction (A) and (B) (Eqs. (1) and (2), respectively) at $25\,^{\circ}C$ are $K_A = 1.7 \times 10^{-2}$ mol and $K_B = 6.2 \times 10^{-7}$ mol, respectively. Therefore, the latter reaction can be neglected under normal conditions. The forward and backward reaction rate constants, for the former reaction, are $K_f = 3.4 \times 10^6\,s^{-1}$ and $K_b = 2 \times 10^8\,s^{-1}$. It appears that the rate of hydrolysis reaction of sulfur dioxide in water, is rapid relative to the diffusion process and that the surface of the water film is instantly saturated at the equilibrium concentration upon exposure to gaseous sulfur dioxide. Therefore, the absorption of sulfur dioxide in water may be treated as a physical mechanism. The forward rate constant K_1 has been measured for the reaction that is first order (Kaji et al. [16]). So the following generalized form can represent the reaction:

$$A + JB \xrightarrow{K_1} product \quad (3)$$

which is first order in A.

Now the rate of reaction is given by

$$rate = -r_A = \frac{-dC_A}{dt} = K_{mn}\Phi_L[A]^m[B]^n \quad (4)$$

$$rate = -r_A = K_{mn}(1 - \Phi_G)[A]^m[B]^n \quad (5)$$

So from Eq. (4), one gets

$$-r_A = \frac{-dC_A}{dt} = k_1\Phi_L C_{AL} \quad (6)$$

2.1.2. Absorption

When formulating the transfer term of the species A, one has to consider the possibility of enhancement of mass transfer caused by the reaction in the liquid phase. Danckwerts and Sharma [17] has treated this particular case of an irreversible first order reaction and his result is given by the following expression:

$$R = K_L a\sqrt{1 + M}\left(C_{AL}^* - \frac{C_{AL}}{1 + M}\right) \quad (7)$$

Also

$$\sqrt{M} = \sqrt{\frac{(2/m + 1)D_A K_{mn}[A^*]^{m-1}[B^0]^n}{K_L^2}} \quad (8)$$

Since $m = 1$, $n = 0$, from Eq. (8) we get,

$$M = \frac{K_1 D_A}{K_L^2} \quad (9)$$

2.1.3. Liquid phase balance

The equation of continuity of A for constant ρ and D_L (liquid phase dispersion coefficient) is given by

$$\frac{\partial C_{AL}}{\partial t} + \left(v_r \frac{\partial C_{AL}}{\partial r} + v_\theta \frac{1}{r} \frac{\partial C_{AL}}{\partial \theta} + v_z \frac{\partial C_{AL}}{\partial z} \right)$$
$$= D_L \left(\frac{1}{r} \frac{\partial}{\partial r} \left(r \frac{\partial C_{AL}}{\partial r} \right) + \frac{1}{r^2} \frac{\partial^2 C_{AL}}{\partial \theta^2} + \frac{\partial^2 C_{AL}}{\partial z^2} \right)$$
$$+ K_L a \sqrt{1+M} \left(C_{AL}^{*'} - \frac{C_{AL}}{1+M} \right) - R_A \tag{10}$$

In Eq. (10), the first part on left hand side is for accumulation and the second part is for convective transport. Whereas the right hand side consisted of molecular transport, enhanced mass transfer due to chemical reaction and disappearance of A by chemical reaction.

Now the following conditions exist when axial dispersion model is used.

1. Steady-state flow, so

$$\frac{\partial C_{AL}}{\partial t} \Rightarrow 0 \tag{11}$$

2. No radial (or tangential) variation of concentration (or dispersion). Only axial variation of concentration occurs, so

$$\frac{\partial C_{AL}}{\partial \theta} = \frac{\partial C_{AL}}{\partial r} = 0 \quad \text{also } v_r = v_\theta = 0 \tag{12}$$

3. Assuming $(\partial C_{AL}/\partial z) = (\partial C_{AL}/\partial x)$ where x denotes any axial distance from the bottom of the bubble column. Also assume $V_z = V_L$ = liquid phase velocity which is opposite to the positive z direction, so a $(-ve)$ sign should be multiplied to the second term of the LHS of Eq. (10).

Using the conditions given in Eqs. (11) and (12) and conditions mentioned in Eq. (3), one should get

$$\Phi_L D_L \frac{d^2 C_{AL}}{dx^2} + V_L \frac{dC_{AL}}{dx} + K_L a \sqrt{1+M}$$
$$\times \left(C_{AL}^{*'} - \frac{C_{AL}}{1+M} \right) - K_1 \Phi_L C_{AL} = 0 \tag{13}$$

Now Eq. (13) can be converted into a dimensionless form by introducing the following dimensionless groups:

$$z = \frac{x}{L} \tag{14}$$

$$\bar{y} = \frac{C_{AL}}{C_{AL}^*(z=0)} \tag{15}$$

$$\bar{x} = \frac{x_{AL}^{*'}}{C_{AL}^*} = \frac{x_A}{x_{A0}} \tag{16}$$

However,

$$\frac{dC_{AL}}{dx} = \frac{dC_{AL}}{d\bar{y}} \frac{d\bar{y}}{dz} \frac{d\bar{z}}{dx} = \frac{C_{AL}^*}{L} \left(\frac{d\bar{y}}{dz} \right) \tag{17}$$

And also

$$\frac{d^2 C_{AL}}{dx^2} = \frac{d}{dx} \left(\frac{dC_{AL}}{dx} \right) = \frac{d}{dz} \frac{dz}{dx} \left(\frac{C_{AL}^*}{L} \frac{d\bar{y}}{dz} \right)$$
$$= \frac{C_{AL}^*}{L^2} \left(\frac{d^2 \bar{y}}{dz^2} \right) \tag{18}$$

So substituting the values of dC_{AL}/dx and $d^2 C_{AL}/dx^2$ from Eqs. (17) and (18) into Eq. (13) one gets

$$\Phi_L D_L \frac{C_{AL}^*}{L^2} \frac{d^2 \bar{y}}{dz^2} + V_L \frac{C_{AL}^*}{L} \frac{d\bar{y}}{dz} + K_L a \sqrt{1+M}$$
$$\times \left(C_{AL}^{*'} - \frac{C_{AL}}{1+M} \right) - K_1 \Phi_L C_{AL} = 0 \tag{19}$$

Multiplying both sides of Eq. (19) by $L/V_L C_{AL}^*$ we get

$$\frac{\Phi_L D_L}{V_L L} \frac{d^2 \bar{y}}{dz^2} + \frac{d\bar{y}}{dz} + \frac{K_L a \sqrt{1+M} L}{V_L}$$
$$\times \left(\frac{C_{AL}^{*'}}{C_{AL}^*} - \frac{C_{AL}}{C_{AL}^*(1+M)} \right) - \frac{K_1 \Phi_L L}{V_L} \frac{C_{AL}}{C_{AL}^*} = 0 \tag{20}$$

Eq. (20) can be rearranged to

$$\frac{1}{Pe_L} \frac{d^2 \bar{y}}{dz^2} + \frac{d\bar{y}}{dz} + St_L \left(\bar{x} - \frac{\bar{y}}{1+M} \right) - D_a \bar{y} = 0 \tag{21}$$

Thus, the liquid phase balance equation (in dimensionless form) is given by Eq. (21) subjected to the boundary conditions.

$$\text{At } z = 0, \quad \frac{d\bar{y}}{dz} = 0 \quad \text{and} \quad \bar{x} = 1 \tag{22}$$

Also

$$\text{At } z = 1, \quad \bar{y} = -\frac{1}{Pe_L} \frac{d\bar{y}}{dz} \tag{23}$$

2.1.4. Gas phase balance

The gas phase balance equation can be obtained from the same continuity equation (Eq. (10)). Continuity equation of A in the gas phase for constant ρ_G and D_G (dispersion coefficient, gas phase) is given by

$$\frac{1}{Pe_G} \frac{d^2 \bar{x}}{dz^2} - \frac{d\bar{x}}{dz} - St_G \left(\bar{x} - \frac{\bar{y}}{1+M} \right) = 0 \tag{24}$$

So, the gas phase balance equation (in the dimensionless form) is given by Eq. (24) subjected to the boundary conditions.

$$\text{at } z = 0, \quad \bar{x} = 1 + \frac{1}{Pe_G} \frac{d\bar{x}}{dz} \quad \text{and} \quad \frac{d\bar{y}}{dz} = 0 \tag{25}$$

and

$$\text{at } z = 1, \quad \frac{d\bar{x}}{dz} = 0 \quad \text{and} \quad \bar{y} = -\frac{1}{Pe_L} \frac{d\bar{y}}{dz} \tag{26}$$

2.2. Model parameter estimation

The model equations developed on the basis of axial dispersion model, described in the previous section, contain a number of independent hydrodynamic and transport parameters. These parameters determine the performance of the bubble column scrubber. The best correlation available in the literature for these parameters has been given below.

1. Gas hold up (Akita and Yoshida [18])

$$(\Phi_G) = \alpha \left[\frac{d_R^2 P_L g}{\sigma_L} \right]^{1/8} \left[\frac{g d_R^3 P_L^2}{\mu_L^2} \right]^{1/12} \frac{V_G}{\sqrt{g d_R}} \tag{27}$$

where $\alpha = 0.2$ for pure liquid and non-electrolytic solutions.

And $\alpha = 0.25$ for salt solutions.

2. Dispersion coefficient (Deckwer et al. [19]), liquid phase

$$D_L = 0.678 d_R^{1.4} V_G^{0.3} \tag{28}$$

where

$$d_R^{1.4} V_G^{0.3} < 400$$

3. Dispersion coefficient (Mangartz and Pilhofer [20]), gas phase

$$D_G = 50 d_R^{1.5} \left(\frac{V_G}{\Phi_G} \right)^3 \tag{29}$$

4. Volumetric liquid mass transfer coefficient (Akita and Yoshida [18])

$$(K_L a) = 0.6 \frac{D_A}{d_R^2} \left(\frac{\mu_L}{P_L D_A} \right)^{0.5} \left(\frac{g d_R^2 P_L}{\sigma_L} \right)^{0.62}$$

$$\times \left(\frac{g d_R^3 P_L^2}{\mu_L^2} \right)^{0.31} \Phi_G^{1.1} \tag{30}$$

5. Interfacial area per unit volume (Schumpe and Deckwer [21])

$$a = 48.7 \left(\frac{V_G}{\mu_L} \right)^{0.51} \tag{31}$$

2.3. Solution of gas phase and liquid phase balance equations using finite difference technique

2.3.1. Gas phase balance equation

$$\frac{1}{Pe_G} \frac{d^2 \bar{x}}{d\bar{z}^2} - \frac{d\bar{x}}{d\bar{z}} - St_G \left(\bar{x} - \frac{\bar{y}}{1 + M} \right) = 0 \tag{32}$$

With boundary conditions

1. At $z = 0$

$$\frac{d\bar{x}}{d\bar{z}} = Pe_G(\bar{x} - 1) \tag{33}$$

and

$$\frac{d\bar{y}}{d\bar{z}} = 0 \tag{34}$$

2. At $z = 1$

$$\frac{d\bar{x}}{d\bar{z}} = 0 \tag{35}$$

and

$$\frac{d\bar{y}}{d\bar{z}} = -Pe_L \bar{y} \tag{36}$$

We know

$$\bar{x}'' = \frac{\bar{x}_{i+1} - 2\bar{x}_i + \bar{x}_{i-1}}{\Delta \bar{z}^2} \tag{37}$$

$$\frac{d\bar{x}}{d\bar{z}} = \frac{[\bar{x}_{i+1} - \bar{x}_{i-1}]}{2 \times \Delta} \tag{38}$$

Now taking four grid points, i.e. $N = 3$ and $i = 1, 2, 3, 4$ we will get the following.

For $i = 1$

$$\frac{1}{Pe_G} \frac{\bar{x}_2 - 2\bar{x}_1 + \bar{x}_0}{(\Delta z) \times (\Delta z)} - \frac{\bar{x}_2 - \bar{x}_0}{2 \times (\Delta z)} - St_G \left[\frac{\bar{x}_1 - \bar{y}_1}{1 + M} \right] = 0 \tag{39}$$

For $i = 2$

$$\frac{1}{Pe_G} \frac{\bar{x}_3 - 2\bar{x}_2 + \bar{x}_1}{(\Delta z) \times (\Delta z)} - \frac{\bar{x}_3 - \bar{x}_1}{2 \times (\Delta z)} - St_G \left[\frac{\bar{x}_2 - \bar{y}_2}{1 + M} \right] = 0 \tag{40}$$

For $i = 3$

$$\frac{1}{Pe_G} \frac{\bar{x}_4 - 2\bar{x}_3 + \bar{x}_2}{(\Delta z) \times (\Delta z)} - \frac{\bar{x}_4 - \bar{x}_2}{2 \times (\Delta z)} - St_G \left[\frac{\bar{x}_3 - \bar{y}_3}{1 + M} \right] = 0 \tag{41}$$

For $i = 4$

$$\frac{1}{Pe_G} \frac{\bar{x}_5 - 2\bar{x}_4 + \bar{x}_3}{(\Delta z) \times (\Delta z)} - \frac{\bar{x}_5 - \bar{x}_3}{2 \times (\Delta z)} - St_G \left[\frac{\bar{x}_4 - \bar{y}_4}{1 + M} \right] = 0 \tag{42}$$

Using boundary conditions (1)

$$\bar{x}_2 - \bar{x}_0 = 2\Delta z \times Pe_G \times [\bar{x}_1 - 1] \tag{43}$$

or

$$\bar{x}_0 = \bar{x}_2 - 2 \times \Delta z \times Pe_G \times [\bar{x}_1 - 1] \tag{44}$$

Also using boundary conditions (2)

$$\bar{x}_3 = \bar{x}_5 \tag{45}$$

Substituting x_0 from Eq. (44) in Eq. (39), one gets

$$\frac{\bar{x}_2 - 2\bar{x}_1 + \bar{x}_2 - 2 \times \Delta z \times Pe_G[\bar{x}_1 - 1]}{Pe_G \times \Delta z \times \Delta z} - St_G \left[\frac{\bar{x}_1 - \bar{y}_1}{1 + M} \right]$$

$$- \frac{2 \times \Delta z \times [\bar{x}_1 - 1] \times Pe_G}{2 \times \Delta z} = 0 \tag{46}$$

Rearranging the Eq. (46) and substituting $x_5 = x_3$, results

$$\left[\frac{-2}{Pe_G \times \Delta z \times \Delta z} - \frac{-2}{\Delta z} - Pe_G - St_G\right]x_1 + \left[\frac{2}{Pe_G \times \Delta z \times \Delta z}\right]x_2 + \left[\frac{St_G}{1+M}\right]y_1 = -\left[\frac{2}{\Delta z} + Pe_G\right] \tag{47}$$

$$\left[\frac{1}{Pe_G \times \Delta z \times \Delta z} + \frac{1}{2 \times \Delta z}\right]x_1 + \left[\frac{-2}{Pe_G \times \Delta z \times \Delta z} - St_G\right]x_2 + \left[\frac{1}{Pe_G \times (\Delta z)^2} - \frac{1}{2 \times \Delta z}\right]x_3 + \left[\frac{St_G}{1+M}\right]y_2 = 0 \tag{48}$$

$$\left[\frac{1}{Pe_G \times \Delta z \times \Delta z} + \frac{1}{2 \times \Delta z}\right]x_2 + \left[\frac{-2}{Pe_G \times \Delta z \times \Delta z} - St_G\right]x_3 + \left[\frac{1}{Pe_G \times (\Delta z)^2} - \frac{1}{2 \times \Delta z}\right]x_4 + \left[\frac{St_G}{1+M}\right]y_3 = 0 \tag{49}$$

$$\left[\frac{2}{Pe_G \times \Delta z \times \Delta z}\right]x_3 + \left[\frac{-2}{Pe_G \times \Delta z \times \Delta z} - St_G\right]x_4 + \left[\frac{St_G}{1+M}\right]y_4 = 0 \tag{50}$$

2.3.2. Liquid phase balance equation

Similar to gas phase balance and incorporating proper boundary conditions, the liquid phase balance equation reduced to the following sets of equation.

$$\left[\frac{-2}{Pe_L \times \Delta z \times \Delta z} - \left(\frac{St_L}{1+M} + D_a\right)\right]y_1 + \left[\frac{2}{Pe_L \times \Delta z \times \Delta z}\right]y_2 + St_L x_1 = 0 \tag{51}$$

$$\left[\frac{1}{Pe_L \times \Delta z \times \Delta z} - \frac{1}{2 \times \Delta z}\right]y_1 + \left[\frac{-2}{Pe_L \times \Delta z \times \Delta z}\right] - \left(\frac{St_L}{1+M} + D_a\right)y_2 + \left[\frac{1}{Pe_L \times \Delta z \times \Delta z} + \frac{1}{2 \times \Delta z}\right]y_3 + St_L x_2 = 0 \tag{52}$$

$$\left[\frac{1}{Pe_L \times \Delta z \times \Delta z} - \frac{1}{2 \times \Delta z}\right]y_2 + \left[\frac{-2}{Pe_L \times \Delta z \times \Delta z}\right] - \left[\frac{St_L}{1+M} + D_a\right]y_3 + \left[\frac{1}{Pe_L \times \Delta z \times \Delta z} + \frac{1}{2 \times \Delta z}\right]y_4 + St_L x_3 = 0 \tag{53}$$

$$\left[\frac{-2}{Pe_L \times \Delta z \times \Delta z} - \frac{2}{\Delta z} - Pe_L - \left(\frac{St_L}{1+M} + D_a\right)\right]y_4 + \left[\frac{2}{Pe_L \times \Delta z \times \Delta z}\right]y_3 + St_L x_4 = 0 \tag{54}$$

Eqs. (47)–(54) can be combined to the following set of equations:

$$a_{11}x_1 + a_{12}x_2 + a_{13}x_3 + a_{14}x_4 + a_{15}y_1 + a_{16}y_2 + a_{17}y_3 + a_{18}y_4 = 0 \tag{55}$$

$$a_{21}x_1 + a_{22}x_2 + a_{23}x_3 + a_{24}x_4 + a_{25}y_1 + a_{26}y_2 + a_{27}y_3 + a_{28}y_4 = 0 \tag{56}$$

$$a_{31}x_1 + a_{32}x_2 + a_{33}x_3 + a_{34}x_4 + a_{35}y_1 + a_{36}y_2 + a_{37}y_3 + a_{38}y_4 = 0 \tag{57}$$

$$a_{41}x_1 + a_{42}x_2 + a_{43}x_3 + a_{44}x_4 + a_{45}y_1 + a_{46}y_2 + a_{47}y_3 + a_{48}y_4 = 0 \tag{58}$$

$$a_{51}x_1 + a_{52}x_2 + a_{53}x_3 + a_{54}x_4 + a_{55}y_1 + a_{56}y_2 + a_{57}y_3 + a_{58}y_4 = 0 \tag{59}$$

$$a_{61}x_1 + a_{62}x_2 + a_{63}x_3 + a_{64}x_4 + a_{65}y_1 + a_{66}y_2 + a_{67}y_3 + a_{68}y_4 = 0 \tag{60}$$

$$a_{71}x_1 + a_{72}x_2 + a_{73}x_3 + a_{74}x_4 + a_{75}y_1 + a_{76}y_2 + a_{77}y_3 + a_{78}y_4 = 0 \tag{61}$$

$$a_{81}x_1 + a_{82}x_2 + a_{83}x_3 + a_{84}x_4 + a_{85}y_1 + a_{86}y_2 + a_{87}y_3 + a_{88}y_4 = 0 \tag{62}$$

Eqs. (55)–(62) can be represented in the matrix form as shown.

$$\begin{bmatrix} a_{11} & a_{12} & a_{13} & a_{14} & a_{15} & a_{16} & a_{17} & a_{18} \\ a_{21} & a_{22} & a_{23} & a_{24} & a_{25} & a_{26} & a_{27} & a_{28} \\ a_{31} & a_{32} & a_{33} & a_{34} & a_{35} & a_{36} & a_{37} & a_{38} \\ a_{41} & a_{42} & a_{43} & a_{44} & a_{45} & a_{46} & a_{47} & a_{48} \\ a_{51} & a_{52} & a_{53} & a_{54} & a_{55} & a_{56} & a_{57} & a_{58} \\ a_{61} & a_{62} & a_{63} & a_{64} & a_{65} & a_{66} & a_{67} & a_{68} \\ a_{71} & a_{72} & a_{73} & a_{74} & a_{75} & a_{76} & a_{77} & a_{78} \\ a_{81} & a_{82} & a_{83} & a_{84} & a_{85} & a_{86} & a_{87} & a_{88} \end{bmatrix} \times \begin{bmatrix} x_1 \\ x_2 \\ x_3 \\ x_4 \\ y_1 \\ y_2 \\ y_3 \\ y_4 \end{bmatrix} = \begin{bmatrix} 0 \\ 0 \\ 0 \\ 0 \\ 0 \\ 0 \\ 0 \\ 0 \end{bmatrix} \tag{63}$$

In matrix form, we get

$$[A][X] = [B] \tag{64}$$

or

$$[X] = [A]^{-1}[B] \tag{65}$$

$$[X] = [\; x_1 \quad x_2 \quad x_3 \quad x_4 \quad y_1 \quad y_2 \quad y_3 \quad y_4\;]^{\mathrm{T}}$$
$$= \text{solution vector} \tag{66}$$

$[A] = [a_{ij}]$, a coefficient matrix (a square matrix of the order of 8); $i = 1, 2, \ldots, 8$ and $j = 1, 2, \ldots 8$.

Now, the values of different elements of the matrix $[A]$ have been calculated separately.

2.4. Simulation of model equations

After obtaining the solution of model equations as described in the previous section of this chapter, in the matrix form, i.e.

$$[A] \times [X] = [B] \tag{67}$$

or

$$[X] = [A]^{-1}[B] \tag{68}$$

the model enables the simulation of bubble column for different values of independent variables. In other words, the performance of bubble column scrubber can be evaluated, with the support of a program. The input data required to run the program are the experimental values of gas flow rate, liquid flow rate, inlet concentration of sulfur dioxide and mode of operation. The simulation of the program provides the outlet concentration of sulfur dioxide as well as the profiles of other pertinent variables in the bubble columns.

In order to verify the theoretical model based on various parameters, an attempt has been made to generate experimental data on the scrubbing of SO_2 in the modified multi-stage bubble column for predicting its performance.

3. Experimental setup and technique

Fig. 1 shows the schematic diagram of the experimental setup that is basically a bubble column consisted of a vertical cylindrical perspex column, 0.1905 m in diameter and 2.0 m long, fitted onto a fructo-conical bottom of mild steel. The latter had a divergence angle of 7° and a height of 0.87 m. The minimum diameter of the fructo-conical section was 0.10 m. The vertical cylindrical column was fitted with a total of five hollow disks (three contraction disks and two expansion disks). The expansion and contraction disks had central axial openings of 0.095 and 0.0476 m, respectively. At the bottom most section of the cylindrical column, just above the fructo-conical cone, was fitted an antenna type

of sparger for generating bubbles uniformly throughout the entire cross section of the column. The first contraction disk (rupture disk) was placed 0.26 m above the sparer. The first expansion disk (guide disk) was fitted at a height of 0.52 m above the sparger and the second contraction disk was fitted at a distance of 0.78 m above the sparger. Thus this section (Section II) of the column consisted of two contraction disks separated by an expansion disk. Section III consisted of the contraction disk located at a height of 0.78 cm above the bubble disperser, an expansion disk located at a height 1.05 m and a contraction disk at a height 1.30 m, from the sparger. A 0.50 m clear space was provided above Section III, for allowing time for gas–liquid separation and also to accommodate bed expansion due to bubbly flow. Arrangement was made for the controlled generation of an air and sulfur dioxide mixture of the desired composition and to fed the air–SO_2 mixture at the base of the cylindrical vertical column so that the effect of the flow pattern changes due to the contraction and expansion disks can be studied. The vertical cylindrical column was fitted with a total of five hollow disks of different openings.

The air–SO_2 mixture, in composition similar to that existing in the exhaust of a coal fired thermal power plant using coal with 0.5% sulfur content, was generated by mixing air and SO_2 in an air-jet ejector (E) assembly. Compressed air from the compressor (CA) was used as the motive fluid in the ejector to aspirate and thoroughly mix air with the SO_2 from the SO_2 gas cylinder (GC). The ejector was mounted with a downward slope of 30° with the air nozzle perfectly aligned along the axis of the ejector throat to ensure an axially symmetrical jet. The air nozzle was fixed at a projection ratio (which is the ratio of the distance between the nozzle tip and the beginning of the parallel throat to the throat diameter), of 3.78 m, which was determined experimentally for obtaining the highest possible mass ratio of the aspirated gas. Compressed air at the desired motive pressure and flow rate was forced through the air nozzle and regulated by a valve (V_4). Simultaneously, the SO_2 was routed at a controlled rate through SO_2 gas regulator and into the ejector. The air and SO_2 gas mixed intensely in the mixing throat of the ejector and the mixture was fed into the sparger fitted at bottom of the vertical column.

In the actual experiment, water was continuously fed at the top of the column and withdrawn at the bottom at such a rate that a particular liquid height and bubble volume can be maintained in the column. In order to collect representative samples, SO_2 gas samples were withdrawn at an approximately iso-kinetic rate. Samples at point S_1 and S_2 were drawn at the rate of $(1–2) \times 10^{-3}$ N m^3/min to match the experimental gas flow rate and the conditions of iso-kinetic sampling. The SO_2 absorption experiments were conducted at gas flow rates of $(1.20–5.46) \times 10^{-3}$ N m^3/s and a liquid flow rates of $(34.48–175) \times 10^{-6}$ m^3/s. Under steady state operating conditions, the SO_2 gas samples were collected at source point S_1 and S_2 with the help of midget impingers (IB) and aspirator bottles. The gas samples were analyzed
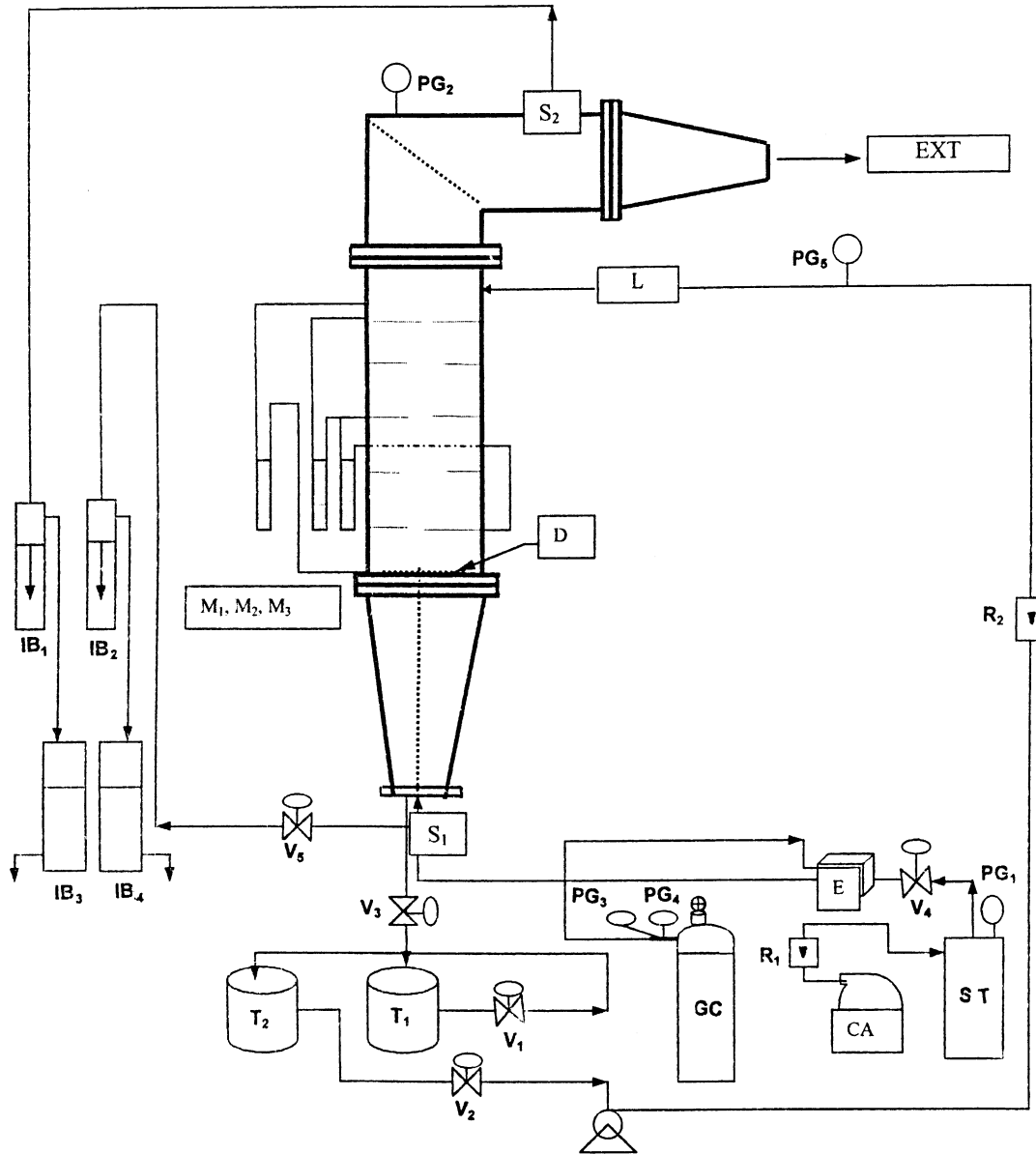
Fig. 1. Schematic diagram of the experimental setup for the scrubbing of SO_2 in water in a MMSBCS. CA: compressor; D: sparger; E: ejector assembly; EXT: exhaust; GC: SO_2 gas cylinder; IB_{1-4}: imping. bubbler; L: water inlet; M_{1-3}: manometers; PG_{1-5}: pressure gauge; R_{1-2}: rotameter; S_{1-2}: source point; T_{1-2}: tank; V_{1-5}: valve.

for sulfur dioxide by the "tetrachloro mercurate method" [22]. The method consisted of passing a portion of the air sampled, through a solution of absorbing medium (sodium tetra-chloro mercurate) and analyzing the resulting solution spectrophometrically (UV–VIS recording spectrophotometer, Model No. UV-2100, Shimadzu, Japan). This method is consisted of calibration of spectrophotometer which can detect 0.001 ppm level of SO_2 concentration as per Indian standards.

Experiments have been conducted by setting the sparger to a condition to generate 2–5 mm range of bubble SMDs (by visual observation), with liquid flow rate of 34.48 × 10^{-6}, 68.95 × 10^{-6}, 103.44 × 10^{-6}, 137.9 × 10^{-6}, 172.4 × 10^{-6} and 206.9 × 10^{-6} m^3/s. Corresponding to each liquid flow rate, gas flow rates of 3.031 × 10^{-3}, 3.640 × 10^{-3}, 4.248 × 10^{-3}, 4.856 × 10^{-3}, 5.462 × 10^{-3} and 6.062 × 10^{-3} N m^3/s have been used. For each liquid flow rate, the inlet SO_2 loading were varied from 600 to 1500 ppm in five stages, e.g. 600, 800, 1000, 1200 and 1500 ppm. The inlet loading was determined by sodium tetrachloro mercurate method as described earlier. Percentage removal of SO_2 have been calculated for each experimental run by the following formula:

$$\eta_{SO_2} = \frac{C_{SO_{2,i}} - C_{SO_{2,o}}}{C_{SO_{2,i}}} \times 100 \qquad (69)$$

. Results and discussions

The trend of the variation of percentage removal have been plotted in a typical plot Fig. 2 for the various inlet loading of SO_2, and for the various operating and flow variables of the bubble column scrubber. The trend of variation of SO_2 removal has also been plotted in the figure along the height of the scrubber.

4.1. Effect of gas flow rate and SO_2 loading on the percentage removal of SO_2

The percentage removal efficiency of SO_2 (η_{SO_2}) at different inlet SO_2 loading and for a constant height of the bubble column scrubber, have been plotted against gas flow rates in Fig. 2. It can be seen from the figure that the percentage removal of SO_2 in the MMSBCS is very high, due to the continuous bursting, reformation and regeneration of bubbles along the vertical height of the column. Very high values of fractional gas holdup, specific interfacial, etc. as reported by Meikap [23], supports these high values. The percentage removal also increases very slightly with the increase in the gas flow rate, for constant liquid flow rates. The increase in the percentage removal of SO_2, with the increase in gas flow rate results from the increased turbulence in the gas phase and higher relative velocity of the gas–liquid interface. It is also interesting to note that beyond a certain value of gas flow rate, e.g. $Q_G = 4.25 \times 10^{-3}\,N\,m^3/s$, the percentage removal of SO_2, remains almost constant.

Fig. 3. Effect of liquid flow rate on percentage removal of SO_2 at constant gas flow rate, $Q_G = 3.031 \times 10^{-3}\,N\,m^3/s$ and for various inlet SO_2 loading. $C_{SO_2,i} = 600, 800, 1000, 1200, 1500\,ppm$.

4.2. Effect of liquid flow rate and SO_2 loading on percentage removal of SO_2

The effect of liquid flow rate, Q_L, on the percentage removal of SO_2, η_{SO_2}, has been presented in Fig. 3 at various inlet SO_2 concentrations, and for constant gas flow rates. It can be seen from the figures that percentage removal of SO_2, η_{SO_2} increases as the liquid flow rate is increased. In the present investigation, as the liquid flow rate is increased the bubble–water interfacial contact area increases. As a result of this, the percentage removal increases with increase in liquid flow rate. In addition, the faster removal of materials from the bubble surface by the downward flowing liquid also helps in the enhancement of SO_2 removal. Thus, increasing liquid flow rate may not increase the total number of bubbles but affect positively the efficiency of individual bubbles, as long sufficient total interfacial area is available in the system. It is also revealed from Fig. 3 that at liquid flow rate of $170 \times 10^{-6}\,m^3/s$, the percentage removal is almost 99.8% at a gas flow rate of $3.031 \times 10^{-3}\,N\,m^3/s$ and at inlet SO_2 loading of 1500 ppm.

4.3. Effect of scrubber height on outlet loading of SO_2

Fig. 4 is a typical plot of the outlet loading of SO_2 versus the height of the scrubber, at constant liquid and gas flow rates, for the different inlet SO_2 loading. It is seen from this figure that the outlet loading of SO_2 decreases exponentially

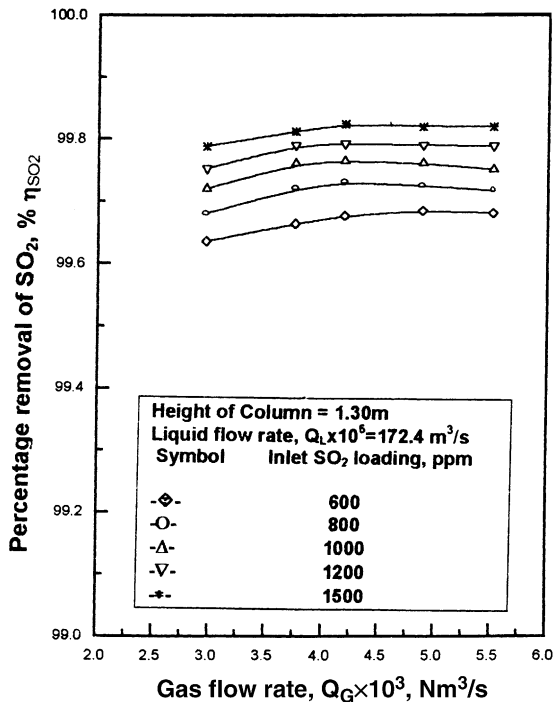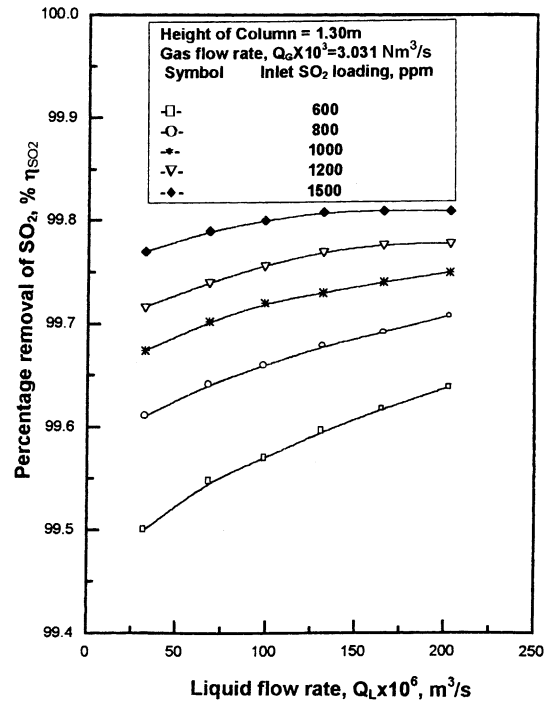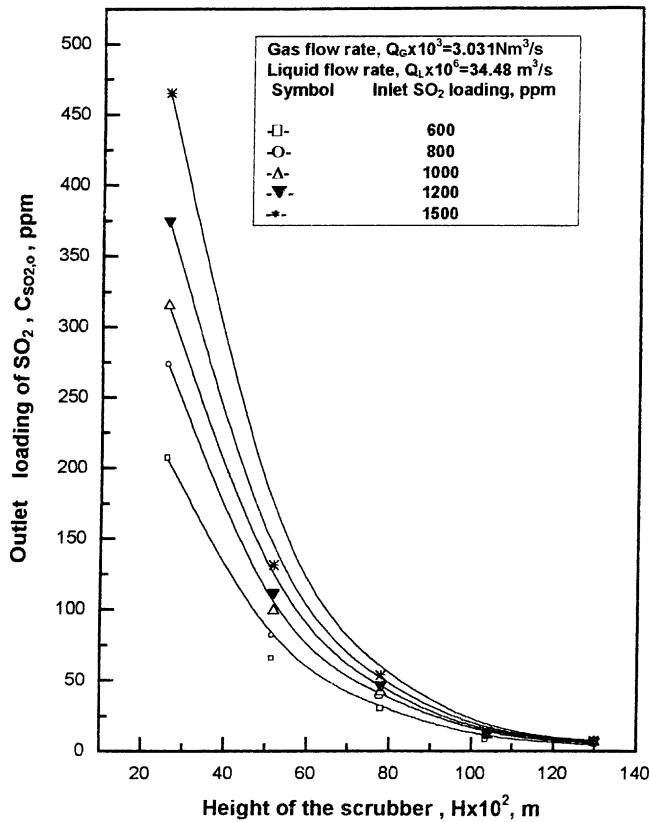Fig. 2. Effect of gas flow rate on the percentage removal of SO_2 for SO_2 scrubbing at various inlet SO_2 loading, $C_{SO_2,i} = 600, 800, 1000, 1200, 1500\,ppm$ and liquid flow rate, $Q_L = 172.4 \times 10^{-6}\,m^3/s$.

Fig. 4. Effect of scrubber height on the outlet concentration of SO_2 at various inlet SO_2 loading.

as the height of scrubber increases. It has also been seen that the outlet SO_2 loading becomes constant after a scrubber height of 1.30 m. Furthermore, similar plots were obtained at different inlet SO_2 loading and it may be seen from these figures that higher values of outlet loading of SO_2 are obtained with higher values of inlet SO_2 loading at constant height of scrubber.

4.4. Model verification

The axial dispersion model proposed in previous section has been used to evaluate the percentage removal of SO_2 in the bubble column from the following equation:

$$1 - \left(\frac{x_A}{x_{A0}}\right) = \frac{(x_{A0} - x_A)}{x_{A0}} \quad \text{or} \quad (1 - \underline{x}) \qquad (70)$$

The values of the percentage removal of SO_2 under the different operating conditions have been presented in Figs. 5 and 6 and the experimentally determined values have also been presented in the same figures. Experimental results indicate that the theoretical equations based on physical mass transfer predict very closely the removal efficiencies obtained with the simple bubble column. It may also be seen from these figures that a very high percentage removal of SO_2 can be achieved from air–SO_2 mixture in the
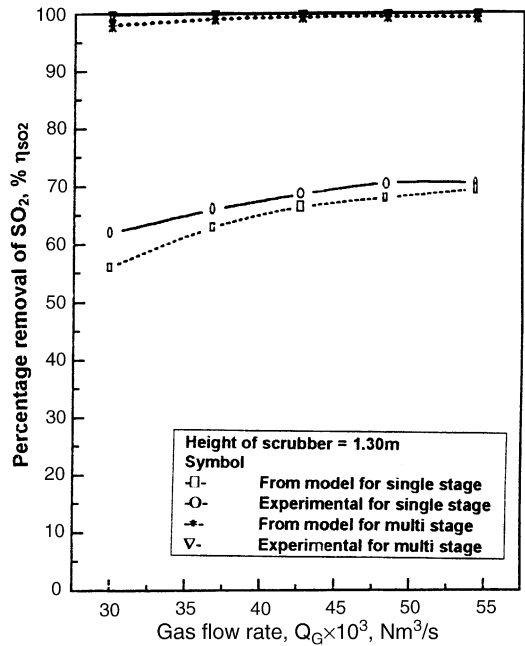

Fig. 5. Comparison of experimental percentage removal efficiency of SO_2 with predicted from model at various gas flow rate.

modified multi-stage bubble column without using any additives or pre-treatment. This high efficiency is attributed to the multi-stage operation. For modified multi-stage bubble column, the experimental results shows clearly the staging
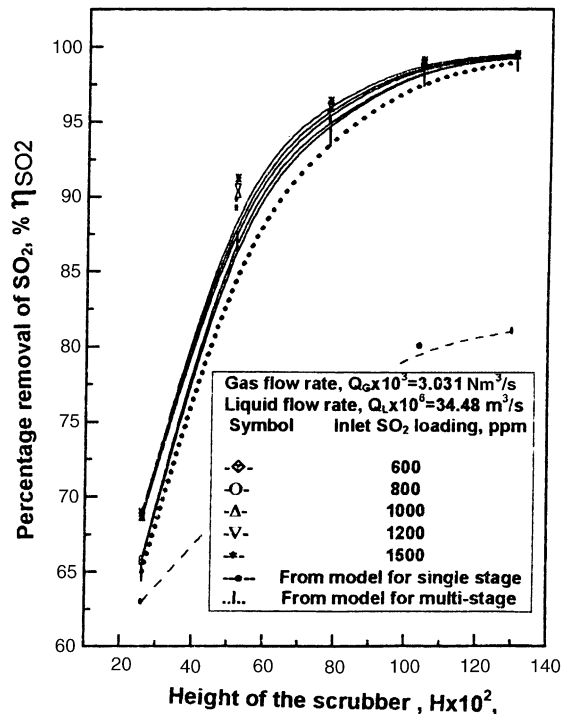

Fig. 6. Comparison for effect of scrubber height on the percentage removal SO_2 loading at various inlet SO_2 loading for SO_2–water system with experimental values and predicted from model.

effect, which leads to almost 100% removal efficiency. The multi-stage Eq. (71) derived from single stage bubble column operation in series which shows that the individual stage efficiencies obtained in the present column were in the range of 83–86%, which is quite close to that predicted by the theoretical model.

$$\eta_T = \eta_1 + (1 - \eta_1)\eta_2 + [1 - (\eta_1 + (1 - \eta_1)\eta_2]x\eta_3 \quad (71)$$

where η_1, η_2, η_3 are the stage efficiency. Thus efficiency, η of around 85% in each stage leads to a overall efficiency 99.2%.

5. Conclusions

A simple but realistic model is developed for the absorption of SO_2 in a MMSBCS. Experimental results indicate that the theoretical equations based on physical mass transfer predict very closely the performance with the simple bubble column for scrubbing of SO_2 using water as the scrubbing medium. Experimental investigation shows that a very high percentage removal of SO_2 can be achieved from air–SO_2 mixture in the modified multi-stage bubble column without using any additives or pre-treatment. This high efficiency is attributed to the multi-stage operation. For modified multi-stage bubble column, the experimental results show clearly the staging effect, which leads to almost 100% removal efficiency. Thus, the present model fits very well for scrubbing of SO_2, which is experimentally verified.

References

[1] R. Higbie, Rate of absorption of a pure gas into a still liquid during short periods of exposure, Trans AIChE 31 (1935) 365.
[2] P.H. Calderbank, C.A. Lochiel, Mass transfer coefficients, velocities and shapes of carbon dioxide bubbles in free rise through distilled water, Chem. Eng. Sci. 19 (1954) 485.
[3] R. Shinner, Chemical reactor modelling, the design and achievable, in: Chemical Reaction Engineering Reviews, Houston, ACS Sypm. Ser., Washington DC, 1978, 1.
[4] J.E. Burman, G.L. Jameson, Diffusional mass transfer to a growing bubble, Chem. Eng. Sci. 31 (1976) 401.
[5] J.L. Huckaby, A.K. Ray, Absorption of sulfur dioxide by growing and evaporating water droplets, Chem. Eng. Sci. 44 (1989) (2797).
[6] S.B. Han, P.W. Park, Absorption from a rising bubble of sulfur dioxide in pure water, Int. Chem. Eng. 30 (1990) 308.
[7] K. Terasaka, H. Tsuge, Bubble formation under constant flow conditions, Chem. Eng. Sci. 48 (1993) 3417.
[8] W. Bronikowska, K. Rudzinski, Absorption of SO_2 into aqueous system, Chem. Eng. Sci. 46 (1991) 2281.
[9] B. Schmidt, E. Stichlmair, Two-phase flow and mass transfer in scrubbers, J. Chem. Eng. Technol. 14 (1991) 162.
[10] A. Bandyopadhyay, M.N. Biswas, On the control of air pollution from Indian coal fired thermal power plants, a new outlook, Ind. J. Environ. Protect. 15 (1995) 853.
[11] A. Bandyopadhyay, M.N. Biswas, Scrubbing of sulphur dioxide in a dual flow scrubber, Indian Association of Environmental Management (IAEM) 26 (1998) 113.
[12] B.C. Meikap, S. Satyaanarayan, A. Nag, M.N. Biswas, Scrubbing of sulfur dioxide from waste gas stream by horizontal co-current flow ejector system, Indian J. Environ. Protect. 19 (1999) 523.
[13] K. Teraska, Y. Hieda, H. Tsuge, Sulfur dioxide bubble formation at an orifice submerged in water, J. Chem. Eng. Jpn. 32 (1999) (472).
[14] V.L. Glomba, Michal, Method for removing sulfur dioxide and fly ashes from boiler flue gases, US Patent (1999).
[15] J. Dohmann, F.A. Mian, M. Iqbal, K. Keldenich, Process for removal of pollutants and trace impurities from flue gas, US Patent (1999).
[16] R. Kaji, Y. Hishinuma, H. Kuroda, SO_2 absorption by water, J. Chem. Eng. Jpn. 18 (2) (1985) 169.
[17] P.V. Danckwerts, M.M. Sharma, Chemical methods of measuring interfacial area and mass transfer coefficient in two fluid systems, Br. Chem. Eng. 15 (1970) 522.
[18] K. Akita, F. Yoshida, Gas holdup and volumetric mass transfer coefficient in bubble columns, Ind. Eng. Chem. Process Des. Dev. 12 (1973) 76.
[19] W.D. Deckwer, R. Burckhart, G. Zoll, Mixing and mass transfer in tall bubble columns, Chem. Eng. Sci. 29 (1974) 2177.
[20] K.H. Mangartz, T.H. Pilhofer, Untersuchungen Zur Gasphasendispersion in Blasensavlenreacktoren, Verfahrenstechnik (Mainz.) 14 (1980) 40.
[21] A. Schumpe, W.D. Deckwer, Gas hold-up, specific interfacial area and mass transfer coefficient at aerated CMC solutions in a bubble column, Ind. Eng. Chem. Proc. Des. Dev. 21 (1982) 706.
[22] Indian Standard, Methods for Measurement of Air Pollution, Sulfur Dioxide, Part VI, IS: 5182, 1969, pp. 4–12.
[23] B.C. Meikap, Abatement of particulate laden SO_2 in modified multi-stage bubble column scrubber, Ph.D. thesis, Indian Institute of Technology, Kharagpur, India, 2000, p. 176.